Solvation Dynamics of Rhodamine 700 in the Nematogenic Liquid Octylcyanobiphenyl

J. Rau, C. Ferrante, F. W. Deeg,* and C. Bräuchle

Institut für Physikalische Chemie, Ludwig-Maximilians-Universität München, Sophienstrasse 11, D-80333 München, Germany

Received: July 17, 1998; In Final Form: November 6, 1998

An investigation of the solvation dynamics of rhodamine 700 in the isotropic phase of the nematogenic substance octylcyanobiphenyl is presented. The time-resolved dynamic Stokes shift $S(t)$ was measured above the nematic−isotropic phase transition and at two temperatures below it. At all temperatures $S(t)$ is characterized by a fast and a slow component on a 10 and 100 ps time scale, respectively. The slow component shows an exponentially activated temperature dependence analogous to the one observed in polar liquids. The fast component exhibits a distinctly different temperature dependence. It is temperature independent from the nematic−isotropic phase transition temperature to 20 K above the transition temperature. Only at higher temperatures does this decay becomes faster. These fast dynamics are associated with the specific anisotropic potential in the locally ordered nematogenic liquid. Additional measurements of the reorientational dynamics of the chromophore are compared with the solvation dynamics investigations.

Introduction

In the past decade a lot of work has been done in the field of solvation dynamics. The motivation underlying it is the study of the influence that different solvents can exert on chemical reactions. Solvent dynamics monitors the solvent behavior when the local electric field experienced by the solvent is suddenly changed. This effect can be achieved for example by exciting a solute molecule from its ground to its excited state, inducing a change in the dipole moment carried by the solute. A similar effect will take place in case of a chemical reaction. Up to now a thorough investigation has been carried out on the solvation dynamics properties of different classes of simple liquids such as polar, hydrogen bonding, and nonpolar, but highly polarizable ones mainly at room temperature.[1−4] Apart from very fast vibrational and librational relaxations on the femtosecond time scale, the investigations on polar liquids have shown that the solvation dynamics are governed by dielectric relaxation on the picosecond time scale.[5,6] The solvent is regarded as a nonstructured environment characterized by macroscopical constants. There is no inherent length scale in these models of solvation dynamics.[7,8] The relaxation of nonpolar liquids is more complex.[4,9−11] It is explained in terms of structural relaxation which is understood as breaking and reformation of the solvent structure. The interaction solute−solvent is not of electrostatic but mechanical nature.

Our main interest is to extend the study of solvation dynamics to more complex liquids such as liquid crystals. For a long time it has been known that pseudonematic domains exist in the isotropic phase of these substances. The presence of these domains is clearly evident in reorientational dynamics as seen, for example, in optical Kerr effect (OKE) measurements of pentylcyanobiphenyl (5CB),[12] N-(4-methoxybenzylidene)-4-*n*-butylaniline (MBBA),[13] and octylcyanobiphenyl (8CB).[14] Right above the nematic−isotropic phase transition these domains are characterized by an orientational correlation length of the order of 10 molecular lengths decreasing to 2−3 molecular lengths 30 K above the phase transition. The temperature dependence of the reorientational time constant associated with these pseudonematic domains up to 30 K above the phase transition is well described by the Landau−de Gennes theory[15] for phase transitions of weakly first-order. This theory predicts a critical behavior approaching the phase transition which was indeed observed in the OKE measurements. The first motivation for our measurements of solvation dynamics in the isotropic phase of a liquid crystal doped with a chromophore was to investigate the sensitivity of the solvation dynamics to the long-range correlation characterizing the pseudonematic domains.

As a second feature the OKE measurements on liquid crystals in the isotropic phase showed a contribution to reorientational dynamics which is 3 orders of magnitude faster than that associated with the collective motions of the pseudonematic domains. This contribution is temperature independent in the temperature range in which the Landau−de Gennes theory is valid. These dynamics are attributed to reorientation inside the domains but are not yet fully understood. The only theory predicting a temperature-independent component in liquid crystals was developed by Sengupta et al.[16]. In it the dynamics are analyzed in terms of the fluctuation modes of pseudonematic domains corresponding to length scales from a molecular size to the domain correlation length. Temperature-independent behavior is predicted to take place on small length scales. Consequently it should be possible to observe these local relaxations by means of solvation dynamics measurements.

In this paper we present the results of our solvation dynamics measurements for the system rhodamine 700 (Rh700) in the isotropic phase of the liquid crystal octylcyanobiphenyl (8CB).

To characterize it solvation dynamics investigations were performed with the fluorescence up-conversion technique. The solvation dynamics are monitored by transient Stokes shift measurements while reorientational dynamics are observed via time-resolved fluorescence anisotropy.[17]

In the next section we will introduce the system we have investigated and describe the instrumental setup. To analyze

* Author to whom correspondence should be addressed. E-mail: fwdeeg@olymp.phys.chemie.uni-muenchen.de.

10.1021/jp983059p CCC: $18.00
Published on Web 01/27/1999

our data we follow the procedure proposed by Maroncelli.[1] Its application to our system together with our results will be presented in Data Analysis and Results. At the end of the section we present also the analysis of the reorientational data. The Discussion section is dedicated to the discussion of our results.We analyze the temperature dependence of the relaxation time for the solvation dynamics of our system in the isotropic phase approaching the nematic−isotropic phase transition and compare the solvation relaxation times with reorientational data obtained from OKE measurements on a solution of 5CB in *n*-heptane. A comparison is also made with the results obtained with the OKE experiments on pure 5CB, and a possible relation to the theory of Sengupta and Fayer is discussed. A summary and concluding remarks are given in the last section.

Experimental Section

The liquid crystalline material 8CB (4′-*n*-octyl-4-cyanobiphenyl) was purchased from MERCK England and was used without further purification. Besides the isotropic phase, the phase mainly investigated in our measurements, 8CB forms a nematic phase between 306.5 and 313.5 K, a smectic A phase between 294.5 and 306.5 K, and a crystalline phase below 294.5 K. The purity of the liquid was tested by the agreement of the measured nematic−isotropic phase transition temperature with the value listed in the literature.[18]

The ionic dye Rh700 (rhodamine 700, counterion perchlorate) was purchased from Radiant Dyes and used as received. For all measurements, solutions of a concentration of $\sim 5 \times 10^{-4}$ M were used. All measurements were performed in quartz sample cells of 1 mm optical path length.

The absorption spectra were recorded with an Uvikon 860 spectrometer from Kontron Instruments with a resolution of 1 nm. The sample was heated by means of a water-thermostat and the temperature was controlled by a Cr/Al-thermoelement (precision $\pm$ 0.5 °C).

The measurements of solvation dynamics and rotational dynamics were performed using the fluorescence up-conversion technique. To investigate the solvation dynamics the time-resolved fluorescence is detected at different wavelengths under magic angle configuration. The rotational dynamics are independent of wavelength, but the spectra have to be recorded separately for parallel and perpendicular polarization of the excitation beam with respect to the detected light. We employed for both experiments the same fluorescence up-conversion design analogous to the setup presented, for example, by Fleming et al.[19].

As excitation source, a DCM dye laser (SP 3500 model) was used synchronously pumped by the compressed and frequency-doubled IR-pulses of a cw mode-locked Nd:YAG laser. At the selected excitation wavelength of 650 nm the pulses were characterized by a pulse width of 500 fs and an average power of 120 mW at the repetition rate of 76 MHz. For the fluorescence up-conversion experiments the output of the dye laser was divided into two beams by a 70/30 beam splitter in order to yield the excitation (70%) and the gate pulse. The excitation pulse was focused by means of a 50 mm lens into a 1 mm quartz cell containing the solution. The fluorescence was collected by a Zeiss Plan Neofluar microscope objective (25/0,60). Since the fluorescence collected by the microscope objective was still divergent, it was recollimated by a 75 mm lens. The light was then focused by a 20 mm lens into a 2 mm thick type I $LiIO_3$ (Gsänger/ Germany) frequency-doubling crystal. The gate pulse was sent into a delay line which allowed us to observe the evolution of the fluorescence intensity over 6.7 ns. For the delay line we used a stepper motor (Unidex 11, Aerotech) with 1 μm resolution. The gate pulses as well as the fluorescence were focused into the doubling crystal by the same lens. Intensity and polarization of both beams could be controlled independently through a combination of half-wave plates and polarizers. The highly divergent up-conversion signal was collimated by a set of lenses and focused into a motor-driven double monochromator (Jobin Yvon H10-D) with 1 nm resolution. The light of the selected wavelength was detected by a photomultiplier (Hamamatsu R4632). The excitation beam was chopped at 800 Hz and the signal was sent into a lock-in amplifier (EG&G Model 5209) connected to a computer. Signal averaging was achieved by collecting scans through repeated running of the delay line. Additionally, the program saves every single scan which permits the elimination of scans clearly affected by strong instabilities of the laser source.

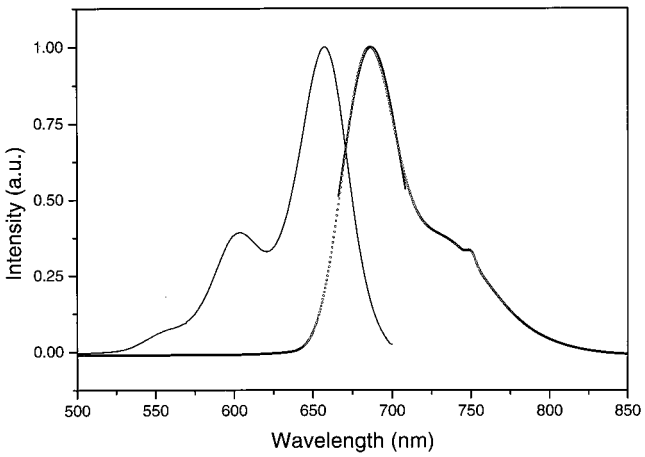

Figure 1. Absorption (full line) and fluorescence (dotted line) of a 5 $\times$ 10^{-4} M solution of Rh700 in 8CB at 325.5 K.

For the steady-state fluorescence spectra the emitted light from the sample was collected by the same microscope objective and sent directly through a set of lenses and mirrors into the monochromator. As detector, a photomultiplier (Hamamatsu R 943-02) characterized by a flat response in the wavelength region of interest was used. Analogous to the fluorescence up-conversion setup the excitation beam was chopped and the signal sent into the lock-in amplifier. The program allowed averaging over several sets of fluorescence spectra. In all measurements the sample was heated by a continuous flow of hot air. The temperature was controlled by a Cr/Al-thermoelement with a precision of $\pm$ 0.5 °C.

Data Analysis and Results

Figure 1 shows the absorption and steady-state fluorescence spectra of Rh700 in 8CB at 333 K. The fluorescence spectrum was recorded by exciting the dye molecule at 650 nm. These spectra were temperature independent in the region of interest. Rh700 which absorbs in a wavelength region above 645 nm was chosen as a chromophore to avoid two-photon absorption of the solvent 8CB showing an absorption band below 320 nm. Two-photon absorption induces undesired heating of the sample. The steady-state fluorescence spectrum is characterized by a main peak at $\lambda = 687$ nm and a shoulder at $\lambda = 733$ nm. In Figure 1 it is also demonstrated that the highest energy transition band can be fitted by a Gaussian function and we used this line

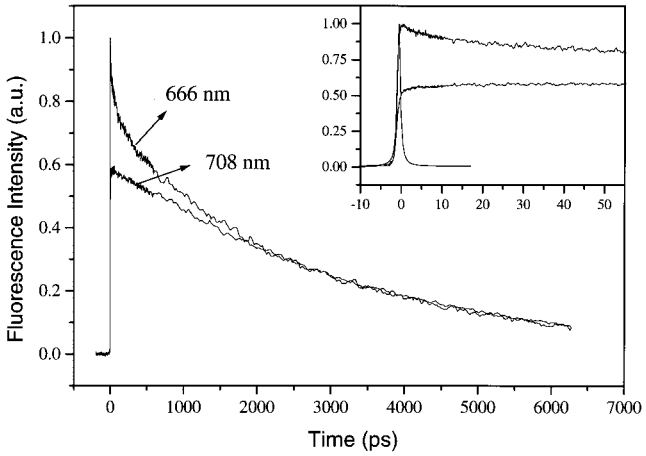

Figure 2. Fluorescence decays of Rh700 5×10^{-4} M in 8CB at 325.5 K and for two different frequencies on the blue (666 nm) and red (708 nm) side of the steady-state fluorescence spectrum. In the inset, together with the two fluorescence decays, the autocorrelation signal of the laser pulses is also shown.

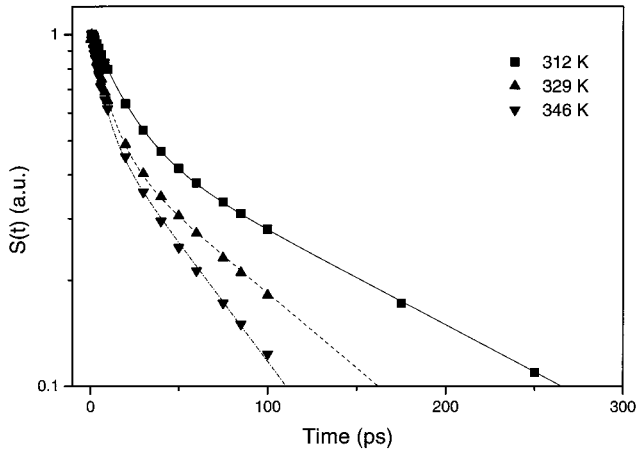

Figure 3. Experimental spectral response function $S(t)$ (see text) for Rh700 5×10^{-4} M in 8CB at three different temperatures. The lines are the result of a double-exponential fit of the $S(t)$ curves.

shape for the procedure of reconstructing the time-dependent fluorescence spectra presented below.

The data analysis is based on the procedure proposed by Maroncelli, so for a detailed discussion we refer to the literature.[1,4,20,21] To monitor the solvation dynamics of Rh700 in 8CB the time-dependent fluorescence decay curves were measured at eight different wavelengths. They were all in the spectral region of the main peak of emission. Figure 2 depicts two typical fluorescence decays in the isotropic phase measured at two wavelengths on the blue ($\lambda = 666$ nm) and on the red ($\lambda = 708$ nm) side of the fluorescence spectrum. From the autocorrelation signal of the pulses recorded at 325 nm and displayed in the inset of Figure 2 we determined a pulse width of 1.5 ps. The decay curves were well described by a triple exponential function. The decay constant of the longest component should reflect the fluorescence lifetime of Rh700. An average of the constants of all longest-lived components allows us to estimate the fluorescence lifetime to be about 3.0 ± 0.3 ns; however, the decay curves could not be reproduced with sufficient precision with this average value. Because of this long lifetime the curves do not decay to zero in the observation time window of 6.7 ns determined by our delay line. The fluorescence spectra at different times were then calculated according to

$$F(\nu,t) = \frac{I(\nu,t)\, I_0(\nu)}{\int_0^\infty I(\nu,t)\, \mathrm{d}t} \tag{1}$$

where $I(\nu,t)$ is the amplitude of the triple exponential fit to the decay curve at the frequency ν and at a time t. Since all decays were measured independently with different laser powers it is necessary to normalize F to the total intensity of the fluorescence. This is achieved by dividing it by the integrated fluorescence intensity. The term $I_0(\nu)$ describes the steady-state fluorescence spectrum which is chosen as the fluorescence reference spectrum. As expected, a systematic movement of the spectra toward smaller wavenumbers was observed with increasing time. In comparison with coumarin dyes[1,20,22] the spectral shift of about 100 cm^{-1} is small, but nevertheless our spectra at different times are clearly distinguishable. Furthermore, the small spectral shift eliminates the problem of reconstruction of the spectra at frequencies where the steady-state fluorescence intensity $I_0(\nu)$ is practically zero. To determine the maximum $\nu_{max}(t)$ of the spectra, the points were fitted with a Gaussian function. The whole analysis was also performed with a log-normal line shape and similar but less consistent results were obtained. We attribute this to the larger number of fitting parameters which were found to be highly dependent from one another.

The time-dependent shift of ν_{max} (t) was fitted with a triple exponential function. $\nu_{max}(0)$ and $\nu_{max}(\infty)$ were obtained by extrapolation of this curve to time zero and time infinity. With the values found for $\nu_{max}(t)$, $\nu_{max}(0)$, and $\nu_{max}(\infty)$ through the Gaussian fits, we calculated the spectral response function $S_\nu(t)$

$$S_\nu(t) \equiv \frac{\nu_{max}(t) - \nu_{max}(\infty)}{\nu_{max}(0) - \nu_{max}(\infty)} \tag{2}$$

The data were fitted again by a triple exponential function and the same time constants as for the decay of $\nu_{max}(t)$ were obtained. The longest component obtained by these fits was characterized by a time constant on the nanosecond time scale and was accounting for only 10% of the total amplitude. Since it was not reproducible by repeated measurements and did not show any systematic behavior as a function of temperature, this longest component has not been further analyzed. This component is subtracted from the values of every data set presented in the following.

The calculated $S(t)$ and the fitted curves are presented in Figure 3 for three different temperatures. The time dependence of $S(t)$ is now well described by a double-exponential function and a clear temperature dependence for the slow component is observed. The temperature dependence determined by fitting the $S(t)$ curves is reported in Figure 4. The time constant increases from 70 ps at 346 K to 165 ps at 312 K. It should be noted that these dynamics are not influenced by the phase transition at T_{NI}. In our figure the points with bars are the average values determined from two different sets of measurements performed at an interval of one month. The upper and the lower limit of the bars are the measured values for the two different sets. Our system is not optimized for measurement in the nematic phase, where the fluorescence light is depolarized by the large number of anisotropic domains. Consequently, the excitation intensity had to be chosen considerably higher in the nematic phase to achieve a sufficient signal-to-noise ratio. Under these conditions we observed decoloration of the sample after several days of excitation. As a consequence, repeated measurements in the nematic phase at 307 K are characterized by a

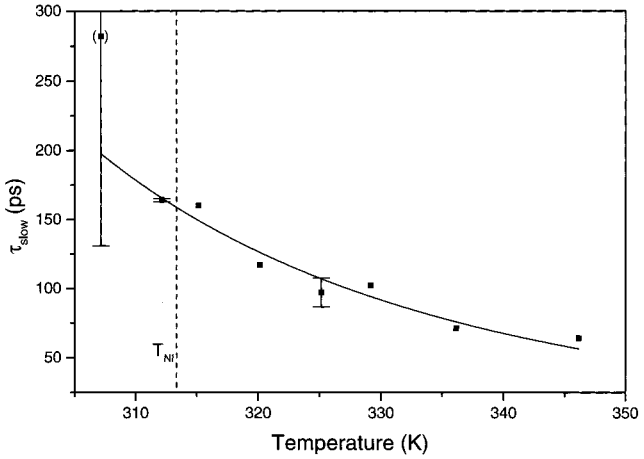

Figure 4. Decay time τ_{slow} (squares) for the slow component of $S(t)$ (see text) as a function of temperature for Rh700 5×10^{-4} M in 8CB. The full line is the result of a fit according to eq 3. The activation energy for the viscosity $E_a = 25 \pm 3$ kJ/mol. The dashed line indicates the temperature T_{NI} at which the nematic−isotropic phase transition occurs.

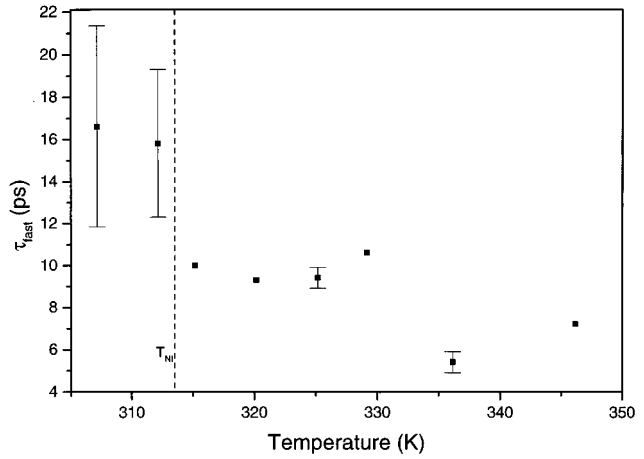

Figure 5. Decay time τ_{fast} (squares) for the fast component of $S(t)$ as a function of temperature for Rh700 5×10^{-4} M in 8CB. The dashed line indicates the temperature at which the nematic−isotropic phase transition occurs.

large error margin. The full line in Figure 4 is the result of a fit of the slow relaxation times τ_s with

$$\tau_s = A\frac{\eta(T)}{T} \tag{3}$$

where $\eta(T)$ is the viscosity of 8CB and T is the temperature. This function predicts the temperature dependence of the solvation dynamics according to the theory of dielectric friction. Further discussion will follow in the next section.

The time constant of the fast component is an order of magnitude smaller than that of the slow component and the temperature dependence, see Figure 5, is different. In the isotropic phase, repeated measurements show that our data have a precision of 1.5 ps which is in the range of our time resolution. Above the phase transition and up to 333 K, we found a constant relaxation time of ∼10 ps; above 333 K the relaxation is faster. As a consequence we did not fit this component according to eq 3. Further arguments for an interpretation of the fast process different from that of the slow one will be discussed in the next section. For reasons discussed above, the data in the nematic phase are less precise. Nevertheless a discontinuity can be

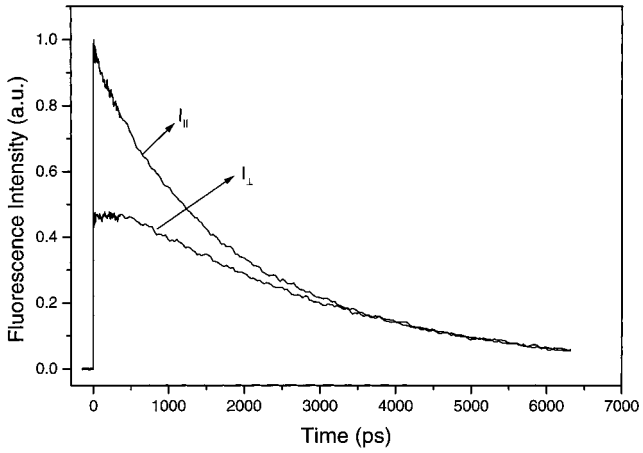

Figure 6. Fluorescence decays measured at parallel (I_{II}) and perpendicular polarization ($I_{\perp}$) for Rh700 5×10^{-4} M in the isotropic phase of 8CB at 360 K.

detected for the fast relaxation time at the phase transition, the two experimental points at 312 and 307 K are both at ∼16 ps.

To obtain a clearer picture of the dynamics connected with the excitation of Rh700 in 8CB we measured the rotational dynamics of the dye molecule in the isotropic phase of 8CB as a function of temperature. Usually this motion is monitored via the time-resolved fluorescence anisotropies $r(t)$[17]

$$r(t) = \frac{I_{II}(t) - I_{\perp}(t)}{I_{II}(t) + 2I_{\perp}(t)} \tag{4}$$

where $I_{II}(t)$ and $I_{\perp}(t)$ are the intensities of the time-resolved fluorescence measured by exciting the system with a polarization parallel or perpendicular to the detected light, respectively. Since $I_{II}(t)$ and $I_{\perp}(t)$ were recorded independently it is necessary to determine their relative intensity to calculate $r(t)$. To this end we used the tail-matching technique which is based on the assumption that for long times both curves decay only with the fluorescence lifetime. One typical pair of curves where tail matching was applied are shown in Figure 6.

The $r(t)$ curves obtained by means of this procedure are normally well fitted by a double exponential function. Since the fast component of these fits has a small amplitude and does not show a consistent behavior as a function of temperature, we preferred to fit the $r(t)$ with a single-exponential function. In Figure 7 the temperature dependence of the relaxation times τ_{or} of the monoexponential fits are presented. The full line in Figure 7 is the result of a fit of our relaxation times with the formula

$$\tau_{or} = B\frac{\eta(T)}{T} \tag{5}$$

where $\eta(T)$ is the viscosity of 8CB and T is the temperature. This temperature dependence is predicted by the Debye−Stokes−Einstein model.

Discussion

In our measurements of solvation dynamics in the isotropic phase of 8CB we observe two distinct relaxation processes. They differ in their respective time scale, 100 ps versus 10 ps, and in their temperature dependence. We will show in the following that the slow component can be described in terms of dielectric relaxation as it is common for polar liquids. The fast process cannot be explained by the same model, since its temperature

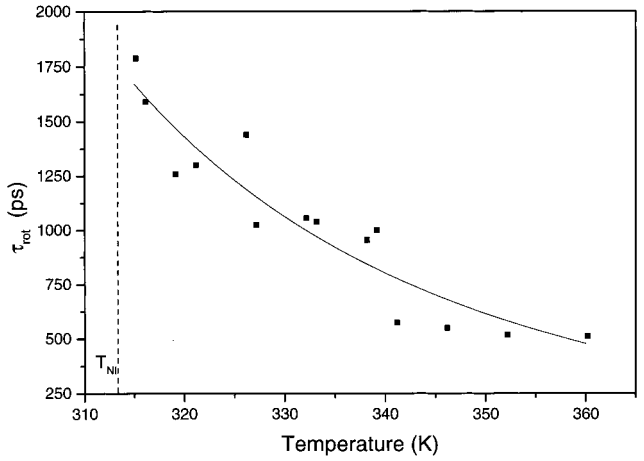

Figure 7. Temperature dependence of the decay time constant of the monoexponential fits of the fluorescence anisotropy $r(t)$ of Rh700 5×10^{-4} M in 8CB. The full line is the result of a fit to eq 5. From the fit E_a (viscosity activation energy) $= 23 \pm 3$ kJ/mol is obtained. The dashed line indicates the temperature at which the nematic−isotropic phase transition occurs.

dependence is not consistent with that predicted by the theory. This behavior will be compared with bulk reorientational dynamics of 5CB in the isotropic phase obtained from OKE measurements.

It has been demonstrated extensively that for polar solvents the spectral shift of the fluorescence spectrum with time can be described in terms of dielectric relaxation. In this theory the solute is considered as a nonpolarizable point dipole centered in a spherical cavity and the solvent is described as a continuum characterized by its dielectric constant. The evolution of the solvation in time is monitored by the frequency dependence of the dielectric constant which for a single Debye dispersion regime is

$$\epsilon(\omega) = \epsilon_\infty + \frac{\epsilon_0 - \epsilon_\infty}{1 - i\omega\tau_D} \tag{6}$$

where ϵ_0 and ϵ_∞ are the static and infinite frequency dielectic constants and τ_D is the Debye relaxation time. The time-dependent Stokes shift is then described,[6,23,24] by a mono-exponential function with a time constant τ_F approximately given by

$$\tau_F = \left(\frac{\epsilon_\infty}{\epsilon_0}\right)\tau_D \tag{7}$$

If the dielectric constant displays more than one distinct dispersion regime several characteristic relaxation times are predicted for solvation dynamics.[24] The temperature dependence for the Debye relaxation time τ_D is given by the Debye−Stokes−Einstein (DSE) relation

$$\tau_D \propto \frac{\eta(T)}{k_B T}$$

$$\eta(T) = \eta_0 \exp(E_a/k_B T) \tag{8}$$

where k_B is the Boltzmann constant, η is the viscosity with activation energy E_a, and T is the temperature. The solid line in Figure 4 is the result of a fit of our data based on eq 8 and an activation energy for the viscosity of 25 ± 3 kJ/mol was obtained. This value is smaller than the one found in the literature of 32 kJ/mol.[18] To check this value and our interpretation we measured the reorientational dynamics of the solute Rh700 in 8CB as well. Since the temperature dependence for such a process should also be described by the DSE relation this experiment gives a second independent value for the activation energy of the viscosity and the resulting activation energy of 23 ± 3 kJ/mol is in good agreement with the solvation dynamics data. The fit is shown in Figure 7 as a solid line.

We have to point out that the interpretation of our results as relaxation governed by dielectric friction is mainly based on the high polarity of 5 D[25] of the 8CB molecules and the existence of a Debye dispersion regime observed in the dielectric measurements. There are also arguments for an interpretation of the slow dynamics in terms of structural relaxation as is observed for nonpolar liquids such as *n*-butylbenzene.[4] Structural relaxation is considered as a process triggered in the solvent by the structural changes induced in the solute following excitation. The dipole in 8CB is mainly localized within the CN group, while the alkylbiphenyl part does practically not contribute to it. The arguments above neglect the influence of this nonpolar group on the solvation process.

We observe a rather small Stokes shift of about 100 cm^{-1} in contrast to the several thousands of wavenumbers observed for Coumarin dyes in polar liquids. There are different possible explanations for it. The Stokes shift of Rh700 in polar liquids such as ethanol is also very small. Consequently we can assume that the change in the charge distribution of Rh700 between its ground- and excited-state configurations is small. On the other side structural relaxation is not directly coupled to the change of the dipole moment, so its influence on the solvation process can increase with decreasing change of the dipole moment of the solute molecule. We were able to investigate the solvation dynamics only over a temperature range of ~30 K, and thus the temperature dependence of the relaxation time cannot be used as a criterion to distinguish between dielectric and structural relaxation. The characteristic time associated with structural relaxation is directly proportional to the viscosity and not to viscosity/temperature.[4] More indirect arguments let us nevertheless attribute the slow component to dielectric relaxation.

Kono et al.[11] have studied the structural and dielectric relaxation in *n*-propanol. According to them the combination of dielectric and structural relaxation result in a nonexponential decay for $S(t)$ which is better described by a stretched exponential. A similar behavior for $S(t)$ was also observed in the study of the solvation dynamics of a nonpolar solute in a nonpolar solvent and the process invoked to explain the data was also structural relaxation.[4] In our case the $S(t)$ curves are well fitted by a double exponential function, while the stretched exponential provided only poor fits. Furthermore McDuffie and Litovitz showed that in *n*-propanol structural relaxation contributes very little compared to dielectric relaxation and is characterized by a time constant fifty times smaller than the dielectric relaxation process.

Another interesting approach to test the validity of our interpretation of the slow relaxation time is to estimate τ_D for 8CB from a different experiment and by means of eq 7, calculate τ_F and compare it with our experimental results.

We cannot extract τ_D from dielectric measurements on pure 8CB, since they are mainly performed in the MHz frequency range and only few data are available in the GHz region.[26,27] The τ_D relaxation time can be evaluated from reorientational measurements performed with the OKE technique.

From a theoretical point of view the reorientational relaxation time τ_R measured with the OKE technique is three times faster than τ_D ($\tau_D = 3\tau_R$). On the other hand, experimental measure-

TABLE 1: Reorientational Relaxation Times from OKE-experiments of 5CB in *n*-Heptane Compared with the Solvation Dynamics Results

η/T (cp/K)	τ_{R1}[(a)] (ps)	τ_{R2}[(a)] (ps)	τ_{F1}(calcd)[(b)] (ps)	τ_{F2}(calcd)[(b)] (ps)	τ_F(meas)[(c)] (ps)
2×10^{-2}	1000	167	295	49	50
5×10^{-2}	3000	413	884	122	100
8×10^{-2}		659		194	150

[(a)] τ_{R1}, τ_{R2} reorientational times of 5CB in *n*-heptane extrapolated to the viscosity of pure 8CB. [(b)] τ_{F1}, τ_{F2} calculated solvation times with eq 7. [(c)] τ_F(meas) solvation dynamics results.

ments of τ_D and τ_R performed on nitrobenzene and bromobenzene with the two different techniques have shown that $\tau_D \approx \tau_R$.[28]

For this reason we will insert in eq 7 the τ_R directly obtained by OKE measurements, without multiplying them by the factor three.

Since the OKE measurements of pure 8CB do not give information about single-molecule reorientation, we used the relaxation times Deeg et al.[12] obtained for a 0.66 M 5CB (4′-*n*-pentyl-4-cyanobiphenyl)/*n*-heptane mixture by the same experiment. In these measurements only isolated 5CB molecules couple to the applied electromagnetic field and consequently the induced anisotropy is destroyed by reorientation of the isolated 5CB molecules. We used their results assuming that the reorientational characteristics for 5CB and 8CB are of the same order of magnitude due to their similar chemical structure. Deeg et al. observed two relaxation times for the reorientation of 5CB in *n*-heptane. Both relaxation times are characterized by a DSE behavior as a function of temperature. From their data we extrapolated the relaxation times τ_D to the vicosity/temperature regime of our measurements. Attributing these τ_D values to 8CB we calculated the corresponding τ_F by means of eq 7. The values $\epsilon_0 = 9.5$ and $\epsilon_\infty \approx 2.8$ are the ones reported by Bose et al.[27] for 8CB. The results of this calculation are shown in Table 1. From these values we expect to observe two components with a Debye−Stokes−Einstein temperature dependence on the hundreds of picoseconds time scale. However only one could be extracted clearly from the measured decays. This component is in very good agreement with the calculated τ_{F2} times and consequently consistent with the predictions of dielectric relaxation theory. An experimentally observed slower component on the hundreds of picoseconds to nanoseconds time scale which was already mentioned in the data analysis section was not further analyzed due to its unsystematic behavior concerning its temperature dependence and its large dependence on the fitting time window. The small amplitude and artifacts on this time scale arising from the fit procedure did not allow a more detailed analysis. Therefore a comparison of this component with τ_{F1} is not possible.

It is equally remarkable that the viscosity, to which the solute is sensitive, is practically identical to the macroscopic viscosity. So even this complex solvent can be treated on the short length scale of the solvation dynamics as a continuum characterized by its macroscopic properties.

We have shown that solvation in the isotropic phase of liquid crystals is not sensitive to the collective reorientational dynamics of the pseudonematic domains observed in OKE and light scattering experiments.[25] We did not observe any critical behavior close to the phase transition. This is in agreement with the behavior Saielli et al.[20] found for the system Coumarin 503 in the liquid crystal mixture ZLI 1167. We investigated the solvation dynamics up to temperatures where the pseudonematic domains are characterized by correlation lengths smaller than three molecular lengths and do not observe any peculiar behavior in the temperature dependence. This indicates that the correlation of the molecules inside the domains is not perceived by the solute even at such small correlation lengths as three molecular lengths. Consequently, we believe that the relaxation around the solute is governed by a solvent shell of a smaller length scale than about three molecular lengths.

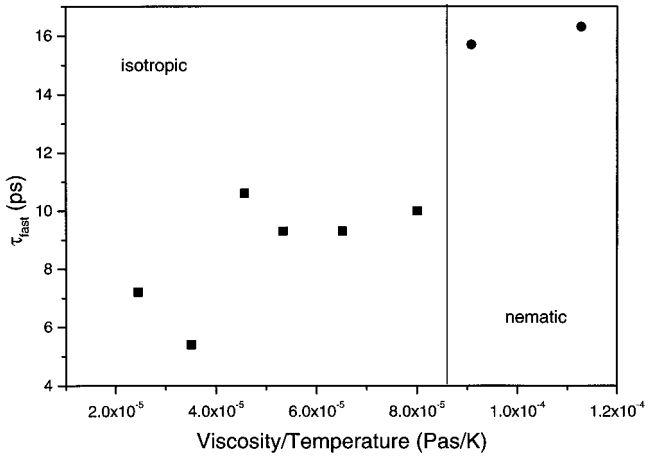

Figure 8. Decay time τ_{fast} for the fast component of $S(t)$ as a function of (viscosity/temperature) for Rh700 5×10^{-4} M in 8CB. The full line separates the data points measured in the nematic (squares) and isotropic (dots) phase, respectively.

We proceed now to discuss the fast process we observed in our solvation dynamics measurements. The presence of faster processes was already suggested by measurements of the dielectric constant of 8CB at high frequencies.[27] Since the dynamics were measured only up to 1 GHz we cannot directly compare our results with theirs. Nevertheless the authors propose as origin of the fast component the existence of dimers in the isotropic phase of 8CB, but there is up to now no experimental proof for the formation of dimers in 8CB (only excimer formation has been observed in fluorescence spectroscopy).

With our measurements we were able to thoroughly investigate the behavior of the fast component as a function of temperature from 307 up to 346 K. In Figure 8 we present the decay times of this fast component as a function of (viscosity/temperature) to outline its non-Debye behavior. The linear dependence of the relaxation time expected from the Debye theory (eq 8) is not fulfilled by the data points in the isotropic phase.

OKE measurements with subpicosecond resolution performed on 5CB and MBBA in the isotropic phase show a somewhat similar behavior. In the pecosecond range the OKE signal measured in these systems is characterized by a strongly nonexponential decay which is (viscosity/temperature) independent up to 30 K above the phase transition. In this context there is remarkable correspondence between the OKE results of 5CB and the solvation dynamics results for 8CB. In both cases the fast component starts to become temperature dependent as the ratio between fast and slow component reaches 1:10.

Up to now there is not yet a complete theory capable of explaining this fast component. We attribute it to reorientational motion of the 8CB molecules inside a static potential due to the presence of a local order of the surrounding solvent molecules. The presence of a pronounced local order in the isotropic phase of liquid crystals has been shown in X-ray-diffraction experiments.[29] If this local ordering also exists around the chromophore, relaxation of molecules within this structured liquid evolves in the potential created by the surrounding

molecules. If the collective dynamics destroying the local structure are on a much longer time scale, a single molecule relaxes in a static potential.

The OKE experiments also support the idea of the influence of pseudonematic domains (i.e., ordered domains) in the isotropic phase of liquid crystals. As such a temperature-independent component is completely absent in the OKE investigations of 5CB dissolved in *n*-heptane,[12] it must be attributed to this local order typical of a nematogenic substance. Sengupta and Fayer[16] have developed a theory which correctly predicts the reorientational dynamics of the pseudonematic domains as well as the temperature-independent relaxation on the faster time scale. An application of this theory to our results is not straightforward, since it would be necessary to define theoretically how these dynamics influence the solvation process which was measured in our experiment. Additionally, in OKE experiments the temperature-independent component is described by a power law decay, while our data show an exponential decay. So at this moment we can only attribute the coincidence of the temperature-independent relaxation to the structure of the solvent, but not to the same relaxation process.

Conclusions

We have investigated the solvation dynamics of Rh700 in the isotropic phase of 8CB. On the basis of our results we have deduced the following picture for the solvation dynamics. There are two distinct processes governing the solvation dynamics between 1 ps and 1 ns. The faster process, characterized by a time scale of 10 ps, is very local and is associated with the specific nematogenic potential created by the surrounding solvent molecules. This process shows a temperature-independent behavior in the isotropic phase up to 20 K above the phase transition temperature. The slower process, characterized by a time scale of 100 ps, fits into the picture of polar solvation and shows the typical temperature dependence for Debye relaxation. At higher temperatures, as the time scales of the two processes become comparable the fast process displays also a temperature dependence. This behavior is not a definite proof of the influence of pseudonematic domains on the solvation process, but it suggests strongly that the specific long-range correlation between the molecules of a liquid crystalline substance affects the solvation process.

Acknowledgment. We thank the Deutsche Forschungsgemeinschaft for financial support of this work under De446/2-2.

References and Notes

(1) Horng, M. L.; Gardecki, J. A.; Papazyan, A.; Maroncelli, M. *J. Phys. Chem.* **1995**, *85*, 784.

(2) Reynolds, L.; Gardecki, J. A.; Frankland, S. J. V.; Horng, M. L.; Maroncelli, M. *J. Phys. Chem.* **1996**, *100*, 10337.

(3) Cichos, F.; Willert, A.; Rempel, U.; von Borczyskowski, C. *J. Phys. Chem. A* **1997**, *101*, 8179.

(4) Fourkas, J. T.; Benigno, A.; Berg, M. *J. Chem. Phys.* **1993**, *99* (*11*), 8552.

(5) Stratt, M.; Maroncelli, M. *J. Chem. Phys.* **1996**, *100*, 12981.

(6) van der Zwan, G.; Hynes, J. T. *J. Chem. Phys.* **1985**, *89*, 4181.

(7) Vajda, S.; Jiminez, R.; Rosenthal, S. J.; Fidler, V.; Fleming, G. R.; Castner, E. W., Jr. *J. Chem. Soc. Faraday. Trans.* **1995**, *91* (*5*), 867.

(8) Sarkar, N.; Datta, A.; Das, S.; Bhattacharyya, K. *J. Phys. Chem.* **1996**, *100*, 15483.

(9) McDuffie, G. E., Jr.; Litovitz, T. A. *J. Chem. Phys.* **1962**, *37* (*8*), 1699.

(10) Litovitz, T. A.; McDuffie, G. E., Jr. *J. Chem. Phys.* **1963**, *39* (*7*), 729.

(11) Kono, R.; Litovitz, T. A.; McDuffie, G. E., Jr. *J. Chem. Phys.* **1966**, *45* (*5*), 1790.

(12) Deeg, F. W.; Greenfield, S. R.; Stankus, J. J.; Newell, V. J.; Fayer, M. D. *J. Chem. Phys.* **1990**, *93* (*5*), 3503.

(13) Stankus, J. J.; Torre, R.; Fayer, M. D. *J. Phys. Chem.* **1993**, *97*, 9478.

(14) Rizi, V.; Ghosh, S. K. *Nouv. Cim.* **1993**, *15D* (*4*), 661.

(15) de Gennes, P. G. *Phys. Lett.* **1969**, *30A*, 454; de Genes, P. G. *Mol. Cryst. Liq. Cryst. (Lett)* **1971**, *12*, 193.

(16) Sengupta, A.; Fayer, M. D. *J. Chem. Phys.* **1995**, *102* (*10*), 4193.

(17) Fleming, G. R. *Chemical Applications of Ultrafast Spectroscopy*; Oxford University Press: New York, 1986.

(18) Kneppe, H.; Schneider, F.; Sharma, N. K. *Ber. Bunsen-Ges. Phys. Chem.* **1981**, *85*, 784.

(19) Castner, E. W., Jr.; Maroncelli, M.; Fleming, G. R. *J. Chem. Phys.* **1987**, *86* (*3*), 1090.

(20) Saielli, G.; Polimeno, A.; Nordio, P. L.; Bartolini, P.; Ricci, M.; Righini, R. *J. Chem. Soc., Faraday Trans.* **1998**, *94* (*1*), 121.

(21) Maroncelli, M.; Fleming, G. R. *J. Chem. Phys.* **1987**, *86* (*11*), 6221.

(22) Jarzeba, W.; Walker, G. C.; Johnson, A. E.; Barbara, P. F. *Chem. Phys.* **1991**, *152*, 57.

(23) Mazurenko, Yu. T. *Opt. Spectrosc. (USSR)* **1974**, *36*, 283.

(24) Baghi, B.; Oxtoby, D. W.; Fleming, G. R. *Chem. Phys.* **1984**, *86*, 257.

(25) Zink, H.; DeJeu, W. H. *Mol. Cryst. Liq. Cryst.* **1985**, *124*, 287.

(26) Duron, C.; Wacrenier, J. M. *J. Phys. (Paris)* **1987**, *38*, 47.

(27) Bose, T. K.; Chahnine, R.; Merabet, M.; Thoen, J. *J. Phys. (Paris)* **1984**, *45*, 1329.

(28) Böttcher, C. J. F.; Bordevijk, P. *Theory of Electric Polarization*, Vol. II, 2nd ed.; Elsevier: Amsterdam, 1978; p 213.

(29) Leadbetter, A. J.; Richardson, R. M.; Colling, C. N. *J. Phys. (Paris)* **1975**, *36*, C1−37.